Cleaner Engineering and Technology 3 (2021) 100097

Contents lists available at ScienceDirect

Cleaner Engineering and Technology

journal homepage: www.journals.elsevier.com/cleaner-engineering-and-technology

Design of magnetic nanotechnological devices for the removal of fluoride from groundwater

Verónica N. Scheverin [a], Analía V. Russo [b,*], María F. Horst [a], Silvia Jacobo [b], Verónica L. Lassalle [a]

[a] INQUISUR, Departamento de Química, Universidad Nacional del Sur (UNS)-CONICET, Av. Alem 1253, 8000, Bahía Blanca, Buenos Aires, Argentina
[b] Laboratorio de Química de Materiales Magnéticos de Aplicación a la Ingeniería (LaQuiMMAI), Facultad de Ingeniería, UBA-IQAI, Av. Paseo Colón 850, C1063ACV, Buenos Aires, Argentina

ARTICLE INFO

Keywords:
Nanocomposites
FLUORIDE
Groundwater
ZEOLITES
MAGNETITE
ADSORPTION

ABSTRACT

The problem associated with water availability embodies a great challenge for scientists and the industrial sector. Groundwater appears as an interesting option to contribute to solving this problem. The natural occurrence of fluoride, among other contaminants, may restrict the widespread use of groundwater. Increasing efforts are dedicated to finding out novel, efficient, green, and low-cost technologies that can solve this inconvenience, being those based on adsorption the preferred ones. In this work, nanocomposites based on natural zeolite and magnetite were synthesized and subsequently superficially modified with aluminum and calcium cations. The main objective is to get surface specificity and functionality for fluoride removal from a real groundwater environment. The raw and modified materials were characterized, aiming to determine their physicochemical as well as stability properties. The crystalline pattern was analyzed by XRD; and the composition by atomic absorption spectroscopy. Besides, FTIR and zeta potential were assayed to identify the functional groups and the surface charge, respectively. Data suggested that surface modification did not affect the crystalline structure of constituent materials. Composition data and FTIR analysis allowed to verify only the aluminum incorporation. Zeta potential evidenced critical changes in modified materials. The adsorption performance of both raw materials and nanocomposites, were tested through batch assays using fluoride model solutions. The first did not show adsorption capacity. As a difference, the surface-modified nanocomposites demonstrated high efficiency, reaching around 90% of fluoride removal. Besides, adsorption assays were replicated employing real groundwater samples from Bahía Blanca (Buenos Aires, Argentina) rural region, achieving greatly satisfactory results when the surface-modified nanocomposites were tested.

1. Introduction

The availability of water for human consumption is considered a critical worldwide issue, representing one of the significant challenges in the future. The growth of the world population, combined with increasing industrial and agricultural activities, have demanded greater water resources. The presence of natural compounds such as heavy metals, arsenic, fluoride, and organic matter limits its availability, at least for human ingestion (Auge et al., 2013).

Fluoride (F^-) is a vital oligo-element required for several functions in live organisms, including humans. However, ingestion of water with high fluoride concentrations may lead to untreatable diseases such as dental and skeletal fluorosis. Thus, the only way to prevent them is to keep fluoride intake within safe limits for human consumption (Sujana et al., 2009).

Reported data suggest that over 200 million people worldwide are exposed to higher fluoride concentrations than those recommended by WHO for drinking water (1.5 mg/L) (Amini et al., 2008; World Health Organization, 2011). The most affected regions are India, China, Central Africa, and South America (World Health Organization, 2011). In this last case, Argentina registers the most serious situation (Ali et al., 2016). In this regard, F^- concentration up to 12 mg/L has been recorded in the central region of Argentina (Gomez et al., 2009). In such place is located Bahía Blanca, a medium-size city from Buenos Aires province (see Fig. 1)

* Corresponding author.
E-mail addresses: veronica.scheverin@uns.edu.ar (V.N. Scheverin), arusso@fi.uba.ar (A.V. Russo), mfhorst@uns.edu.ar (M.F. Horst), veronica.lassalle@uns.edu.ar (V.L. Lassalle).

https://doi.org/10.1016/j.clet.2021.100097
Received 14 November 2020; Received in revised form 20 February 2021; Accepted 8 April 2021

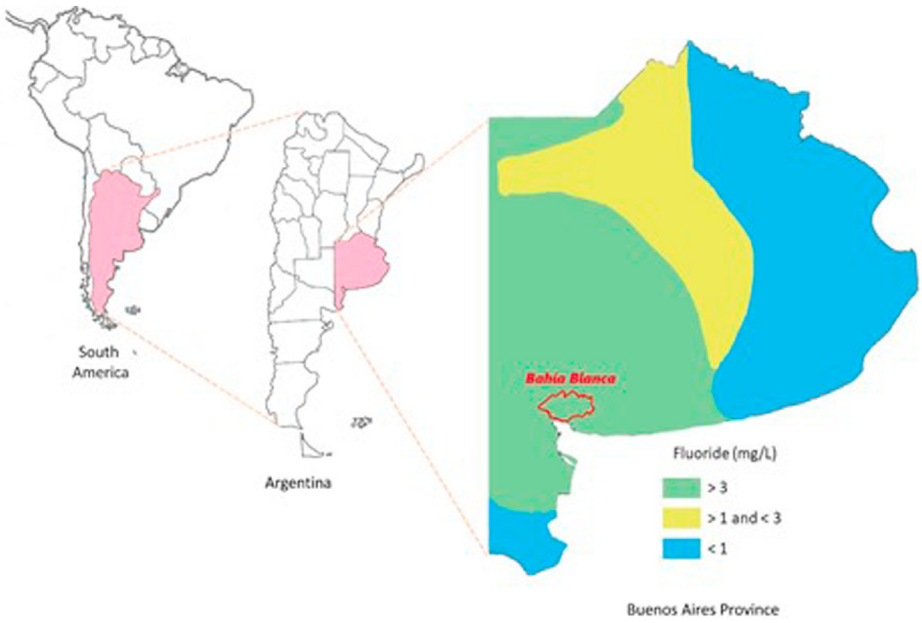

Fig. 1. Geographical location of Bahía Blanca city and the distribution of F^- in the groundwater of the Buenos Aires Province.

where fluoride levels on the order of 3.55–6.69 mg/L have been reported (Al Rawahi, 2016; Ruiz and Francisca, 2017). Earlier articles from, Paoloni et al. have informed values around 4–5 mg/L and even as higher as 17.5 and 18.2 mg/L, depending on the screened zone (Paoloni et al., 2003).

The conventional procedures to overcome these problems involve adsorption, chemical precipitation, ion-exchange, and membrane treatments (Mohapatra et al., 2009). Among these technologies, membrane and ion-exchange processes are hardly implemented in rural areas due to their expensive installation and maintenance costs, while chemical precipitation results in toxic sludge formation with high fluoride concentration (Habuda-Stanić et al., 2014). In this scenario, the adsorption process is considered one of the most suitable considering the compromise cost-effective (Viswanathan and Meenakshi, 2008). The activated alumina (Al_2O_3) is commonly employed as an adsorbent because of its high affinity and selectivity for this element. Nevertheless, the maximum adsorption capacity is reported below pH 6, limiting its direct application in real groundwater treatments where the pH is around 7–8.5 (Habuda-Stanić et al., 2014).

Adsorbents obtained from natural raw sources are currently preferably designed because of their eco-friendly and low-cost properties. Hence, biomaterials such as biochar, clay minerals, iron oxides, zeolites, activated carbon, among others, are being intensely investigated (Bonetto et al., 2015). Zeolites, a kind of natural clays, are microporous crystals with well-defined structures composing by AlO_4 and SiO_4 tetrahedra linked through the common oxygen atoms (Pavelić et al., 2000). Due to its high ion-exchange capacity and stability, they are recognized as efficient adsorbent materials (Delkash et al., 2015). Researchers have studied different kinds of zeolites for the adsorption of various cationic contaminants such as cobalt, zinc, and manganese, from aqueous solutions (Nakhli et al., 2017). For instance, El-Azim et al. explored the use of clinoptilolite to remove cadmium, iron, and nickel (El-Azim and Mourad, 2018). In recent work, Kobashashi et al. studied the adsorption of heavy metals like mercury and lead by zeolites synthesized by fly ash (Kobayashi et al., 2020).

Despite this, the antecedents in open literature concerning zeolite-based compounds for adsorption of anionic species are limited due to the negative surface charge that exhibits these minerals in almost all the pH range (Habuda-Stanić et al., 2014). Several published articles deal with the surface modification of zeolites by employing multivalent metallic cations to sort out the lack of ability to bind anions. Rahmani et al. modified a natural zeolite with Al^{3+}, and Fe^{+3} by ionic exchange to improve adsorption capacity for F^- (Rahmani et al., 2010). Reported results indicate that the modification process raised the ability of zeolites to bind F- from <20% to 76% and 65% when zeolites were modified with Al and Fe, respectively. In another contribution, Teutli-Sequeira et al. informed an increment of F^- uptake when the employed zeolite electrochemically modified with Al in the place of the raw one. In this same sense, other authors have reported that the calcium incorporation on zeolite surface improved its removal capability, reaching about 96.3% concerning raw zeolite efficiency, which was about 9.6% (Zhang et al., 2011). Similar results were reached by the of zeolites with other metals, such as iron (III) (Sun et al., 2011), lanthanum (III) (Viswanathan and Meenakshi, 2008), aluminum (III), and calcium (II) (Waghmare et al., 2015).

Another recognized drawback for zeolites-based adsorbents is associated with their poor reusability capacity because of the difficulties found in separation process. Incorporating of magnetic nanoparticles may be a useful strategy to improve the recuperation, ability, and posterior reuse of zeolite-based adsorbents (Teutli-Sequeira et al., 2013).

In own research, magnetic zeolites adsorbents have been designed and examined to remove arsenic and heavy metals from groundwater from the Bahía Blanca region (Scheverin et al., 2019). However, the mentioned adsorbents lack the affinity to eliminate fluoride from this water source. In this context, the present contribution proposes the subsequent surface modification of magnetic zeolite nanocomposites, aiming to provide them suitable binding sites for removing fluoride (as a model of anionic pollutant) from groundwater. To do this, the surface incorporation of aluminum (Al) and calcium (Ca) cations has been performed. This approach involves the thorough characterization of obtained materials and the study of their ability to remove fluoride, focusing on evaluating the performance of designed materials in real aqueous environments. Specifically, groundwater samples from the region Bahía Blanca (Buenos Aires, Argentina) have been used.

According to the available bibliography, composite materials herein presented have not been explored enough. The few contributions found are mainly based on the study of fluoride removal from model aqueous solutions, avoiding the complexity of a natural water source (Xu et al., 2020). Thus, this work intends to provide a more realistic perspective in terms of the efficiency of magnetic-zeolite nanocomposites for fluoride elimination from groundwater samples.

Table 1
Material denomination.

Material	Description
Z	Natural zeolite
Z-AC	Natural zeolite modified with Al and Ca
ZFe	Natural zeolite loaded with iron zerovalent
ZFe-AC	Natural zeolite loaded with iron zerovalent modified with Al and Ca
M	Raw magnetite
M-AC	Magnetite modified with Al and Ca
MZ	Magnetite-zeolite composite
MZ-AC	Magnetite-zeolite composite modified with Al and Ca

2. Materials and methods

The natural zeolite (Z) was supplied by DIATEC S.R.L., extracted from La Rioja deposit (Argentina). For the synthesis of magnetite-zeolite composite, Z was previously ground and sieved with mesh size of 297 μm.

Ferrous sulfate heptahydrate ($FeSO_4.7H_2O$), sodium hydroxide (NaOH), ferric chloride hexahydrate ($FeCl_3.6H_2O$), aluminum potassium sulfate ($KAl(SO_4)_2$), calcium sulfate ($CaSO_4$) and sodium fluoride (NaF) used in this study were all analytical grade reagents.

2.1. Synthesis of iron zerovalent loaded zeolite

A natural zeolite loaded with zerovalent iron (ZFe) was synthesized according to previous reports (Russo et al., 2014). Briefly, 32 g of Z was immersed in an aqueous solution of $FeSO_4$ (0,14 M) for 24 h. After the exchange procedure, the sample was washed with bidistilled water. The reduction of Fe (II) was carried out by adding KBH_4 solution to an aqueous dispersion of the sample under nitrogen atmosphere. The solid was ground and sieved to obtain a 297 μm size.

2.2. Synthesis of magnetic composite

The magnetic composite was prepared by adapting the previously reported chemical co-precipitation method (Horst et al., 2016). In summary, 100 mL of ferric/ferrous solution with a molar ratio of 2/1 was prepared. Then 1 g of natural zeolite was added. The obtained suspension was stirred at 70 °C for 30 min under a nitrogen atmosphere. Afterward, 25 mL of NaOH 5 M were added at a controlled rate of approximately 1 mL min^{-1} to precipitate the iron oxide. The solid was isolated using a magnet and washed several times with bidistilled water until the supernatant showed conductivity lower than 50 μS. Finally, it was dried in an oven at 41 °C for 48 h. The obtained magnetic composite was named MZ and was extensively characterized and studied in previous work (Scheverin et al., 2019).

2.3. Methodology of Al and Ca incorporation

The natural zeolite (Z), zerovalent iron-loaded zeolite (ZFe), magnetite nanoparticles (M), and magnetite-zeolite composite (MZ) were surface modified by the incorporation of Al and Ca following the methodology reported by Waghmare et al. (2015) with some modifications. Briefly, each material was dispersed into a potassium aluminum sulfate solution for 30 min and then was added to a calcium sulfate solution. Material: $KAl(SO_4)_2$: $Ca(SO_4)$ w/w ratio used was 1:2:0.5, respectively. The pH of the suspension was adjusted in a range 7–8 using NaOH under magnetic stirring for 3 h at room temperature. Solids were isolated by centrifugation or magnetic decantation and dried at 41 °C for 48 h. The identification of the obtained materials is listed in Table 1.

Table 2
Chemical composition of shallow groundwater used for real water adsorption assays.

Parameter	Unit	Value
F	mg/L	14.40
As	mg/L	0.201
Fe	mg/L	0.014
Al	mg/L	0.031
Na	mg/L	626
SO_4^{2-}	mg/L	542
Cl^-	mg/L	260
pH		8.70
Electrical conductivity	mS/cm	4.38

2.4. Characterization

The composition of materials was estimated in terms of iron, aluminum, and calcium content, using atomic absorption spectroscopy (GBC Avanta 932 Spectrometer). A proper amount of material was treated with a HNO_3:HCl ratio of 3:1. All the measurements were conducted by triplicate.

Fourier transformed infrared spectroscopy (FTIR) was employed to identify the surface functional groups of the materials. FTIR spectra were taken on a Thermo Scientific Nicolet iS50 covering the 4000-400 cm^{-1} range. For this purpose, 1 mg of sample was ground with 250 mg of anhydrous KBr and compressed into a pellet used for the spectrum collection.

X-ray diffraction (XRD) analyses were performed to obtain the crystalline structure of all the samples. The assays were recorded by a PANalytical Empyrean 3 diffractometer with a Ni-filtered CuKα radiation, a graphite monochromator, and a PIXcel3D detector. It was operated at a voltage of 45 kV and a current of 40 mA, in the 2Θ range from 5° to 70° using a continuous scan mode with a scan angular speed of 0.016° min^{-1}.

The zeta potential (ζ) was measured in a Malvern Zetasizer Nano ZS90 using dispersions of 1 mg of material mL^{-1} in bidistilled water at pH 8. Every dispersion was sonicated for 30 min previous to the assay.

2.5. Adsorption assays

Adsorption performance of prepared materials was tested by analyzing their ability to retain F^- from aqueous solutions. A series of batch experiments were performed adjusting different test times, ranging from 5 to 180 min, at room temperature. For the experiments, 4 mg of adsorbent/1 mL of a fluoride solution was used. The magnetic composites were separated from the supernatant by magnetic decantation, while materials without magnetic properties were separated by filtration (0.22 μm).

Fluoride concentration was determined indirectly by quantifying it on the supernatants, employing a specific ion electrode. This method includes using a total adjustment buffer solution (TISAB) based on acetic acid, sodium citrate, and sodium chloride. The removal efficiency (%) and equilibrium adsorbed concentration, Qeq (mg/g), were calculated according to the following equations:

$$\%R = (Ci - Cf)\ x\ 100\ /\ Ci$$

$$Qeq = (Ci - Cf)\ xV/M$$

where Ci and Cf are the initial and final concentration of F^- (mg/L), respectively, V is the total volume of solution (L) and M is de adsorbent mass (g).

Two different adsorption assays were performed:

2.5.1. 2.5.1. Model adsorption assays

A stock solution of 6 ppm of fluoride was prepared by dissolving an appropriate amount of NaF in 1000 mL of bidistilled water. The pH solution was adjusted to 8 by adding NaOH 0.1 M to simulate the pH of the real groundwater sample.

Table 3
Composition of the raw and modified materials.

Materials	Fe (mg/g)		Al (mg/g)		Ca (mg/g)	
	average	σ	average	σ	average	σ
Z	0.980	0.08	3.52	0.01	0.193	0.019
ZFe	3.360	1.15	3.84	0.06	[a]	[a]
M	616.4	0.10	[a]	[a]	[a]	[a]
MZ	287.5	0.81	2.34	0.03	0.057	0.001
Z-AC	0.640	0.02	8.29	0.12	[a]	[a]
ZFe-AC	1.570	0.30	8.49	0.01	[a]	[a]
M-AC	323.5	6.73	7.87	0.06	[a]	[a]
MZ-AC	281.9	24.9	78.7	1.95	[a]	[a]

[a] Values below limit of detection (0.05 mg/g).

2.5.2. 2.5.2. Real water adsorption assays

In this case, shallow groundwater collected in Paraje La Hormiga (Bahía Blanca, Buenos Aires, Argentina) was employed as adsorption media. The sample was conserved frozen until the assays. The analysis of the water composition is shown in Table 2. The pH was not regulated for the adsorption experiments.

2.6. Stability assays

The stability of the adsorbent materials was explored in terms of the Fe and Al leaching. The materials were immersed in real water samples, using the same adsorbent/volume of water ratio in model adsorption assays. The modified materials do not contain quantifiable Ca values, and therefore Ca leaching was not studied.

Fe and Al contents in the supernatants were measured by atomic absorption spectroscopy (GBC Avanta 932 Spectrometer) and atomic emission spectroscopy (ICP-AES Shimadzu 1000 mod III), respectively.

3. Results and discussion

The following sections discuss, firstly, the results of the characterization of prepared zeolite-based adsorbents. Then the adsorption assays and finally the reuse and stability of the synthesized materials are discussed.

3.1. Characterizations of adsorbent materials

The composition of raw and Al–Ca modified nanocomposites is shown in Table 3. As expected, the Al content increased when the surface modification is performed. In the cases of Z-AC, ZFe-AC, and M-AC, Al content reached an almost constant value. A different trend was found in MZ-AC, where the Al content resulted in one order of magnitude higher than the other adsorbents. This behavior may be related to the multiple active sites provided by the combination of Z with the iron oxide, and changes in the porosity associated to the inclusion of magnetite nanoparticles. Published reports demonstrated that a rise in magnetic-zeolite nanocomposite porosity leads to improved adsorption properties, regarding its constituent materials (Amodu et al., 2015).

In most of the analyzed adsorbents, the Ca content could not be quantified because it was in a lower concentration than the detection limit (0.05 mg/g) regarding the employed methodology. The obtained results for Z and MZ materials indicate that leaching of calcium occurred during the modification process. This is in accordance with data published by other authors. Teutli-Sequeira et al. reported that, after a similar treatment, the Ca content decreased as the Al content increased in both natural hematite and zeolite (Teutli-Sequeira et al., 2013). This suggests that ion-exchange, occurring by displacement of calcium ions, is one of the mechanisms by which aluminum would be loaded into zeolitic moieties (Guaya et al., 2015).

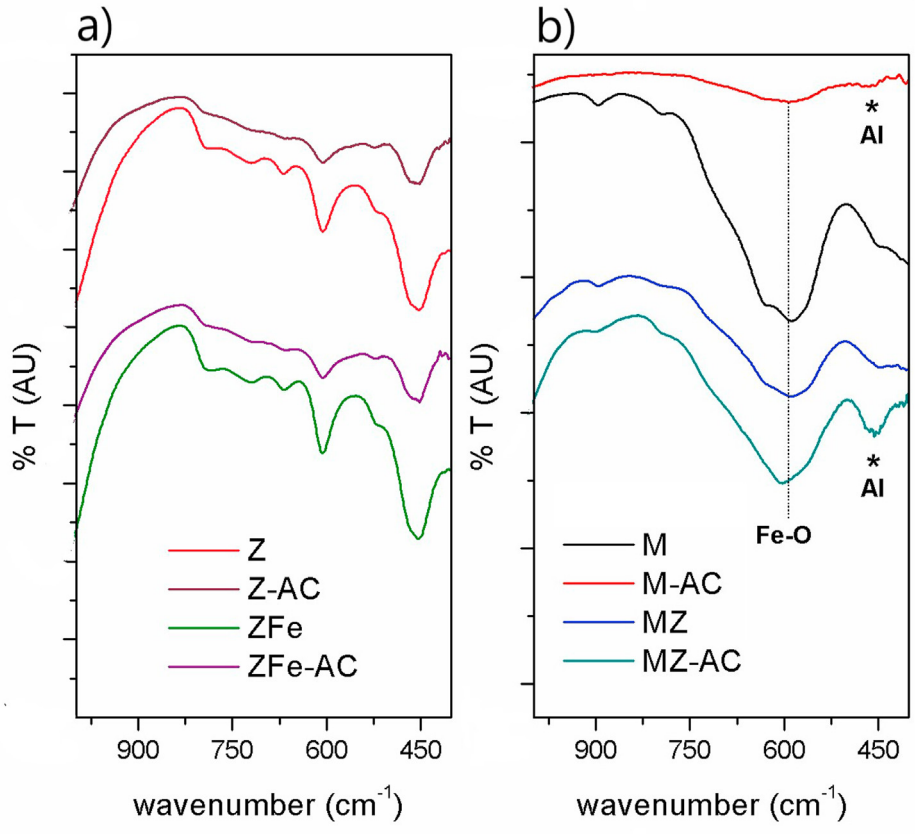

Fig. 2. Region of low wavenumbers of FTIR spectra of a) zeolite-based materials b) magnetic based materials.

Table 4
Assignment of IR bands for raw and modified materials.

Band assignment	Z	Z-AC	ZFe	ZFe-AC	M	M-AC	MZ	MZ-AC
Si–OH–Al	3616.3	–	3624.4	–	–	–	–	–
O–H	3456.2	3454.7	3452.9	3454.4	3431.1	3418.0	3429.9	3445.2
N–H s	–	–	3016.8	–	–	–	–	–
H_2O pa	1634.3	1634.6	1633.7	1634.8	1633.8	1638.4	1632.5	1634.5
N–H b	–	–	1400.7	–	–	–	–	–
SiO_4	1203.4	1206.5	1201.2	1200.7	–	–	1200.1	1209.5
Si–O–Al	1049.0	1054.2	1050.2	1061.8	–	–	1053.4	1065.8
Fe–O	–	–	–	–	592.1	589.3	592.9	602.9
Al–O	–	–	–	–	–	464.9	–	452.6

*s: stretch; b: bending; pc: physically adsorbed.

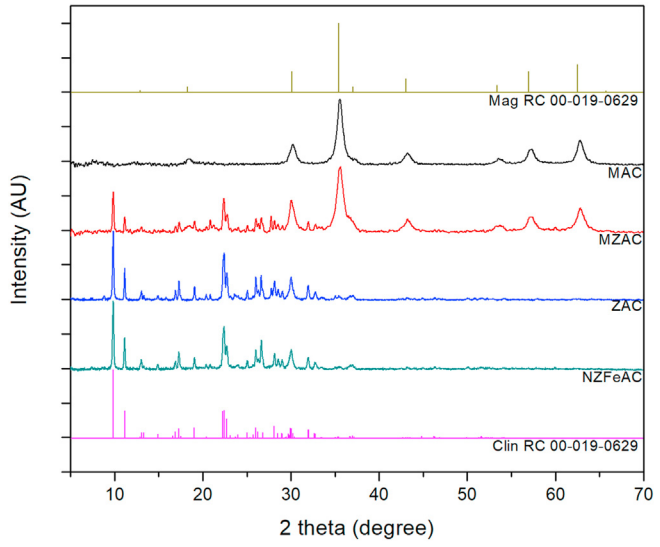

Fig. 3. XRD diffractograms of surface modified materials with the corresponding (Z and M) crystalline patterns as references.

Fig. 2 compares the FTIR spectra of raw and modified materials aiming to evaluate functional and structural changes. Table 4 lists the main spectra bands for the materials. In all analyzed spectra, the band at ~1600 cm^{-1} is related to physically adsorbed H_2O (Salem Attia et al., 2014). In the spectra corresponding to zeolitic materials, the signals associated with the internal vibration of Si–O-T (T = Al; Si) appear in the range of 1200–900 cm^{-1}, while peaks related to internal T-O bond linkages in TO_4 of zeolite lattices, lie between 900 and 400 cm^{-1}. Signals ascribed to OH bridging groups in ≡Si–OH–Al≡ and H–O···H are visualized near 3600 and 3400 cm^{-1}, respectively (Blanco Varela et al., 2006).

The spectra of Z-AC and ZFe-AC evidence significant differences regarding Z and ZFe.

In both cases, the bands associated with the Si–O–Al bond show a shift to higher wavenumbers. This shift may be related to the Al/Si ratio changes after modification (Favvas et al., 2016). These findings are in agreement with those arising from composition analysis (see Table 3). Further proof of Al incorporation may be found from the widening of bands located at wavenumbers lower than 800 cm^{-1}. Other authors have reported similar results with regards to incorporating cations into zeolite frameworks (Mozgawa, 2000). On the other hand, the absence of the band associated to bridging O–H groups in ≡Si–OH–Al≡ is observed. The disappearance of this band indicates that these specific O–H bonds are involved in the Al-Z interactions (Doula, 2007). The FTIR spectrum of ZFe-AC does not show the typical band associated with the presence of N–H groups derived from the synthetic process (Bakatula et al., 2015). This evidence can be ascribed to the complete displacement of ammonium groups for Al ions during the surface modification.

Table 5
Values of zeta potential in bidistilled water, pH 8.

Sample	ζ (mV)	Sample	ζ (mV)
Z-AC	−2.87	Z	−36.9
ZFe-AC	7.26	ZFe	−37.0
M-AC	2.44	M	−25.9
MZ-AC	17.9	MZ	−9.34

Raw magnetite (M) exhibits a well-defined band at 592 cm^{-1}, which can be assigned to typical Fe–O bond. This band is widened and loses definition in the spectrum of M-AC material. Besides, a weak signal appears at 456 cm^{-1}, which could be related to incorporated Al (Waghmare et al., 2015).

The band at 456 cm^{-1} also appears in the MZ-AC spectrum. Besides, it is noticeable the shift of Fe–O band in MZ-AC material concerning MZ. This peak entirely overlaps with those associated with T-O bonds. Then, these changes could be related to Fe···Al or T-O···Al interactions.

In Fig. 3, the diffractograms of modified materials are compared with the magnetite (JCPDS 19–629) and clinoptilolite (JCPDS 39–1383) patterns. The diffractograms reveal that barely perceptible changes are observed in 2θ reflection peaks regarding standard patterns, revealing that the crystalline pattern of Z-AC and ZFe-AC mainly agree with the pattern corresponding to clinoptilolite. The peaks of M-AC correspond to the magnetite pattern. The XRD diffractogram corresponding to the MZ-AC nanocomposite match with the crystalline pattern of magnetite and clinoptilolite. These results suggest that surface modification has not affected the crystalline structure of constituent materials (Waghmare et al., 2015). As described by Guaya et al. the absence of additional diffraction peaks indicates the formation of amorphous oxide/hydroxide of Al (Guaya et al., 2015).

As it is well known, zeta potential (ζ) gives information regarding surface changes in terms of electrical charge. Hence it might be a useful tool to infer qualitatively the composition of the nanocomposites. ζ of all materials was measured by dispersing them in bidistilled water. In these experiments, pH was adjusted to 8 to simulate the behavior of the materials in real groundwater media. The results are listed in Table 5.

The ζ measured values exhibit critical differences between the different adsorbents; hence they may be well considered as proof of the surface modification of the materials. All the assayed materials present ζ positive except Z-AC. This behavior is the expected one considering the incorporation of Al cations to the zeolitic moieties. These findings agree with information reported by other authors referring to zeolite modified with Al and Ca (Waghmare et al., 2015). From these results, it is possible to infer that modified materials have the potential to remove pollutants with a negative charge through electrostatic interactions.

On the other hand, the magnitude of the ζ is commonly employed as a criterion to estimate the colloidal stability of a nanoparticulated dispersion. The higher the absolute value of the ζ, the greater the colloidal stability of the nanosystems in the media when the stabilization mechanism is by electrostatic repulsion. In this sense, MZ-AC has the highest potential value compared to the other modified materials. Therefore, MZ-AC would be the most stable material in a colloidal suspension.

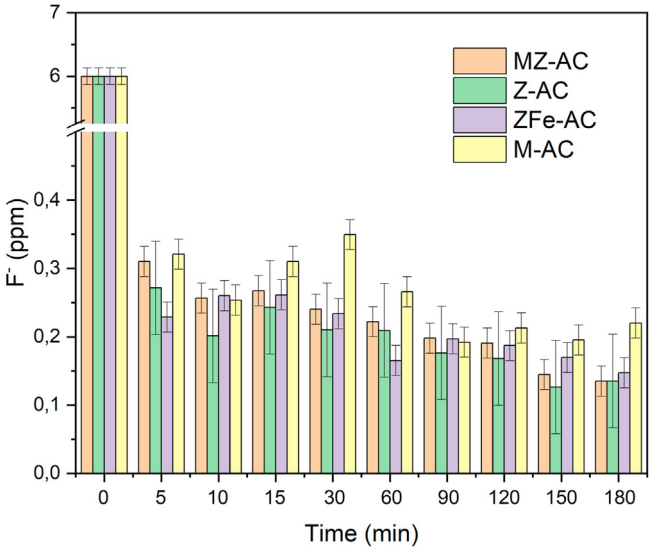

Fig. 4. Decrease in F^- concentration as a function of contact time for the assays performed employing model F^- solution.

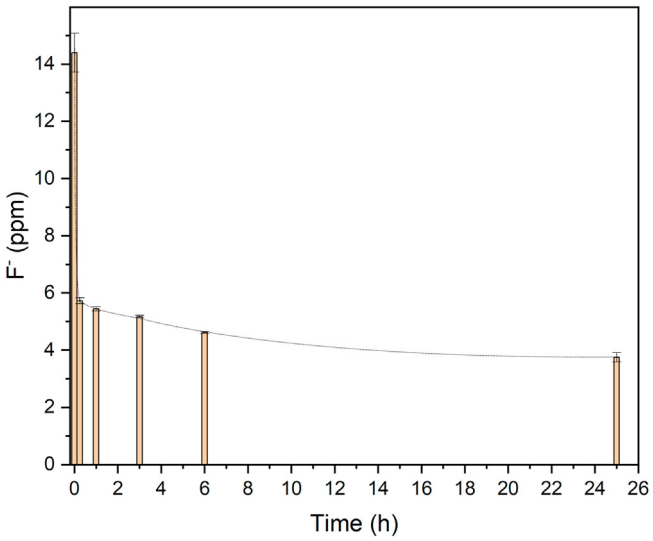

Fig. 5. Kinetic adsorption profile of F^- in MZ-AC using real water sample.

Table 6
Qeq amount and percentage of removal for fluoride adsorption of AC materials in model solution.

Material	Qeq (mg/g)	% Removal
Z-AC	1,46	97,7
ZFe-AC	1,46	97,5
M-AC	1,45	96,3
MZ-AC	1,46	97,7

3.2. Adsorption assays

The efficiency of an adsorption process depends on several factors, such as the initial concentration of adsorbate, contact time, dosage, and surface functionality of the adsorbents. Previous works in the research groups allowed to gain insight regarding the optimal operating conditions employing alike systems (Horst et al., 2016). Hence these aspects were out of the focus of this article whose main goal is to demonstrate the viability of the prepared materials in real environments.

Fig. 4 shows the decrease in F^- concentration as a function of the contact time of the AC materials employing a F^- model solution. The raw materials were not efficient in the explored conditions (data not shown). This behavior could be explained in terms of insufficient contact time and physicochemical properties. Other authors have found similar results. Chang et al. informed that the equilibrium time for magnetite nanoparticles as fluoride adsorbent was 13.5 h (Chang et al., 2006), representing a prolonged time to implement a real treatment system. On the other hand, the capacity of natural zeolites for anion removal is limited because of their extremely negative surface charge (Samatya et al., 2007). As a consequence, different procedures are frequently performed for the activation of zeolites. The most common is the ion-exchange that can improve their adsorption capacity, generating new active sites for fluoride adsorption (Waghmare et al., 2015).

In contrast, the AC materials show high efficiency to remove fluoride (>90%) in model solution during the first minutes of the assay. The average initial pH was 8 ± 0.2 with a mean equilibrium pH of 8.5 ± 0.2. After water treatment, F^- concentration reached lower values than those recommended by the WHO (0.7–1.5 ppm) (World Health Organization, 2011). These results demonstrate and support the hypothesis that surface modification is crucial to ensure the capability of the prepared materials to bind anionic species.

The specific amount of F^- uptake and the removed (expressed as removal percentage) are listed in Table 6. A similar trend has been found for all the prepared materials. Even when Z-AC has negative ζ, its behavior is comparable. The latter implies that the interaction between F^- and the adsorbent occurs not exclusively by electrostatic attraction. The adsorption mechanism of F^- onto aluminum-based composites has been widely reported in the literature (Alhassan et al., 2020); and involves electrostatic interactions and ion-exchange between hydroxyl ion and fluoride, producing a rise of the pH after treatment. The predominance of one over another phenomenon depends on the medium conditions as well as on the surface charge of the adsorbents (Bhatnagar et al., 2011).

From the results achieved, MZ-AC was selected to assess fluoride kinetic studies in a real groundwater sample. This is because of its easy separation from the media through the application of a magnetic field, as well as its further reuse possibility.

The batch experiments were conducted at different points regarding the time, being 180 the maximum contact time, based on previous studies in the research group (Horst et al., 2018). The groundwater used for this assay had an initial fluoride concentration of 14.4 ppm. The pH value was 8.7, and electrical conductivity was (4.38 mS), which is typical of the sampled region (Auge et al., 2013). The chemical composition of the water sample is listed in Table 2.

As observed in Fig. 5, MZ-AC presents fast initial adsorption. Consequently, the water sample registered a fall in the F^- concentration from 14 to 5.73 ppm during the first 15 min, representing 60% of removal. However, in this experiment, the Qeq (2.66 mg/g) was higher than the registered with model solutions (1.46 mg/g). This behavior could be explained considering that with the increase of initial concentration, Qeq increases but the removal percentage decreases (Tran et al., 2017).

Besides higher values of initial F^- concentration compared to the model solutions, the presence of multiple additional species in real water could further contribute to the decline of the fluoride removal percentage. Such species may compete with F^- for the adsorption sites on the surface of MZ-AC. The interference of anionic species in the F^- adsorption into aluminum-based compounds has been reported (Mohapatra et al., 2009). While chloride has a minimal effect on removal efficiency, arsenate, and sulfate severely affect the availability of the reactive sites to bind F^- (Mondal and George, 2015). Waghmare et al. reported that the adsorption capacity of an AC-material decreased by 40% in the presence of various co-anions (Waghmare et al., 2015). Besides, the increment of pH value regarding model solutions could further contribute to a decrease in the percentage of removal (Nie et al., 2012).

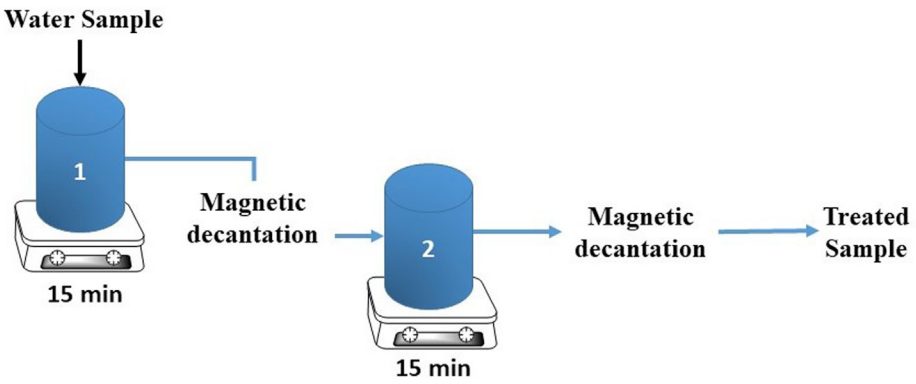

Fig. 6. Scheme of process that involves two consecutive adsorption processes.

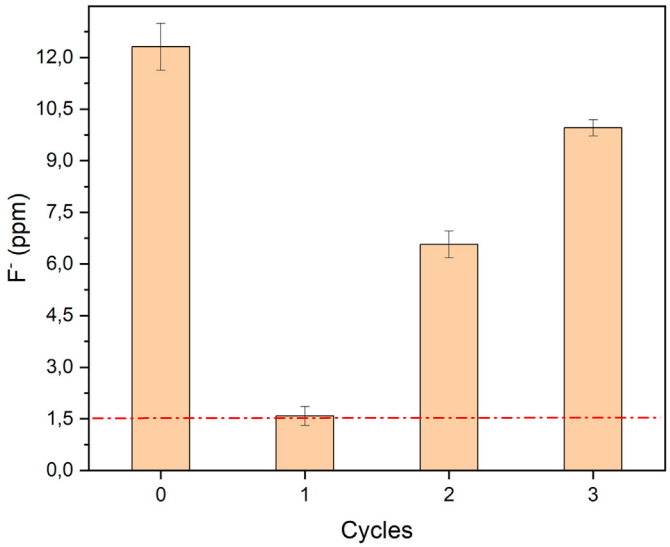

Fig. 7. Cycles of reuse of the purpose process with MZ-AC for F^- adsorption.

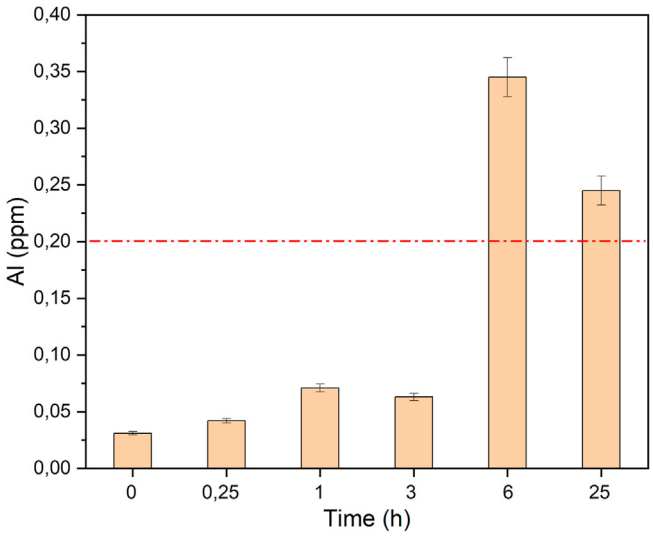

Fig. 8. Residual Al concentration after treatment as a function of time. The dotted line indicates the permitted limit of Al in drinking water.

3.2.1. *Reusability assays*

The real water sample was subjected to a process that involves two consecutive adsorption steps. Fig. 6 shows the scheme of this process. The assay was carried on to improve fluoride removal efficiency with the goal to reach the values allowed by the current regulation (0.7–1.5 ppm). In summary, a sample of real water was incubated with the MZ-AC adsorbent. After 15 min, the treated water was separated by magnetic decantation. Then, the treated water was subjected to a second adsorption step with the same adsorbent. Besides, the reuse of the described process was explored without involving any regeneration/purification step on the adsorbent material.

Fig. 7 illustrates the final fluoride concentration after each process. During the first one, the F^- concentration was reduced to the allowed values, reaching 87.5% of removal efficiency. A considerable decrease in F^- adsorption was observed in the second and third cycles of reuse. From these results, it is evident that MZ-AC quickly saturates, demonstrating the need to explore a desorption step. Several strategies may be implemented to increase the useful life of this adsorbent, aiming to process and purify higher volumes of water. One of them may be regeneration. This could be done using a NaOH solution to improve the removal efficiency of the material and to enhance the utility of these materials in time (Sakhare et al., 2012). Other strategies may be associated with the operational conditions, such as the mass of adsorbent/volume of water ratio or pre-treatment of the water to eliminate possible interfering species (Burris and Juenger, 2016).

3.2.2. *Stability assays*

The presence of residual metals arising from adsorbents used for water treatment is an important issue that is frequently missing in the current studies regarding this topic.

(Mondal and George, 2015). Iron is an essential and not hazardous element in human nutrition, so regulatory information regarding its drinking water presence is hard to find. On the other side, aluminum is associated with a series of neurological diseases, and the allowed limit in drinking water is 0.2 mg/L (World Health Organization, 2011).

The material stability in real water was studied for 25 h to evaluate the possible leaching of iron and aluminum in the supernatant. The results revealed that iron leaching did not occur during the period of the assay. However, an increase in aluminum concentration in the water sample was quantified (Fig. 8), reaching higher values than those recommended by the legislation. The compiled data corresponds to the treatment implemented during 6 h.

From these results, it is evident that MZ-AC would not possess enough stability under times longer than 6 h. This behavior could be associated with the solubility of Al in the presence of high values of fluoride concentration in real water (Mondal and George, 2015). George et al. associated the solubility with the formation of monomeric aluminum fluoride and aluminum hydroxyl fluoride complexes (George et al., 2010). The high pH value in the real sample would also contribute to Al dissolution from MZ-AC material. Chang et al. studied the chemical stability of

aluminum-magnetic adsorbent at different pH values. They found that leaching occurred at pH values above 8 (Chang et al., 2006). Similar behavior was reported by other authors (Nie et al., 2012).

The achieved data suggest that some restrictions may be applied to this adsorbent to eliminate fluoride from groundwater, maintaining its safety concerning human health. One of them is the stability time, lower than 6 h. Another would be related to the range of pH of the water source. It would also be possible to implement a sequential remediation process. This should involve two consecutive adsorption steps on the same sample, avoiding the exposure of the adsorbent to the groundwater samples during extensive periods of time.

4. Conclusions

The surface modification of magnetic-zeolite nanocomposites has been successfully implemented by incorporating Al and Ca moieties. The raw materials and modified nanocomposites were characterized, aiming to determine the physicochemical properties.

The composition analysis data reveals the preferred incorporation of Al cations over the calcium ones. The FTIR data allowed to verify only the aluminum incorporation. XRD analysis shows that surface modification has not affected the crystalline structure of constituent materials. The zeta potential evidenced critical changes in modified materials regarding raw materials, supporting the occurrence of surface modification.

The materials demonstrated to be highly efficient adsorbents for fluoride employing model aqueous solutions. The adsorption performance of the selected adsorbents slightly decreased in real groundwater from the Bahía Blanca region. This could be associated with the specific composition and physicochemical properties of the selected real water sample.

The proposed adsorbents exhibit some restrictions related to their application times in real environments compared with those explored within this work to ensure their safety in terms of the leaching of Al ions. This analysis reveals the strong influence of the origin of water samples concerning their properties (ions concentration, pH, etc.); and points to the need to carefully adjust the treatment methodologies to ensure the stability of the adsorbent material under operational conditions.

Declaration of competing interest

The authors declare that they have no known competing financial interests or personal relationships that could have appeared to influence the work reported in this paper.

Acknowledgements

The authors acknowledge the financial support of UNS, Argentina; CONICET, Argentina; ANPCyT, Argentina.

Lic. V. N. Scheverin acknowledges CIC (Comisión de Investigaciones Científicas de la Provincia de Buenos Aires).

References

Al Rawahi, W., 2016. PhD Thesis. Vanadium, Arsenic and Fluoride in Natural Waters from Argentina and Possible Impact on Human Health, Guildford. University of Surrey, UK, pp. 71–73.

Alhassan, S.I., Huang, L., He, Y., Yan, L., Wu, B., 2020. Technology Fluoride Removal from Water Using Alumina and Aluminum-Based Composites : A Comprehensive Review of Progress 3389.

Ali, S., Thakur, S.K., Sarkar, A., Shekhar, S., 2016. Worldwide contamination of water by fluoride. Environ. Chem. Lett. 14, 291–315. https://doi.org/10.1007/s10311-016-0563-5.

Amini, M., Mueller, K., Abbaspour, K.C., Rosenberg, T., Afyuni, M., Møller, K.N., Sarr, M., Johnson, C.A., 2008. Statistical modeling of global geogenic fluoride contamination in groundwaters. Environ. Sci. Technol. 42, 3662–3668. https://doi.org/10.1021/es071958y.

Amodu, O.S., Ojumu, T.V., Ntwampe, S.K., Ayanda, O.S., 2015. Rapid Adsorption of Crystal Violet onto Magnetic Zeolite Synthesized from Fly Ash and Magnetite Nanoparticles 191–203.

Auge, M., Espinosa, G., Sierra, L., 2013. Arsénico en el agua subterránea de la provincia de buenos aires. VIII Congr. Argentino Hidrogeol. y VI Semin. Hisp. Latinoam. Hidrol. Subterránea 2. https://doi.org/10.13140/RG.2.1.3333.4245.

Bakatula, E.N., Mosai, A.K., Tutu, H., 2015. Removal of uranium from aqueous solutions using ammonium-modified zeolite. S. Afr. J. Chem. 68, 165–171. https://doi.org/10.17159/0379-4350/2015/v68a23.

Bhatnagar, A., Kumar, E., Sillanpää, M., 2011. Fluoride removal from water by adsorption —. A review 171, 811–840. https://doi.org/10.1016/j.cej.2011.05.028.

Blanco Varela, M.T., Martínez Ramírez, S., Ereña, I., Gener, M., Carmona, P., 2006. Characterization and pozzolanicity of zeolitic rocks from two Cuban deposits. Appl. Clay Sci. 33, 149–159. https://doi.org/10.1016/J.CLAY.2006.04.006.

Bonetto, L.R., Ferrarini, F., de Marco, C., Crespo, J.S., Guégan, R., Giovanela, M., 2015. Removal of methyl violet 2B dye from aqueous solution using a magnetic composite as an adsorbent. J. Water Process Eng. 6, 11–20. https://doi.org/10.1016/J.JWPE.2015.02.006.

Burris, L.E., Juenger, M.C.G., 2016. The effect of acid treatment on the reactivity of natural zeolites used as supplementary cementitious materials. Cement Concr. Res. 79, 185–193. https://doi.org/10.1016/j.cemconres.2015.08.007.

Chang, C., Lin, P., Wolfgang, H., 2006. Aluminum-type superparamagnetic adsorbents : synthesis and application on fluoride removal 280, pp. 194–202. https://doi.org/10.1016/j.colsurfa.2006.02.011.

Delkash, M., Ebrazi Bakhshayesh, B., Kazemian, H., 2015. Using zeolitic adsorbents to cleanup special wastewater streams: a review. Microporous Mesoporous Mater. 214, 224–241. https://doi.org/10.1016/j.micromeso.2015.04.039.

Doula, M.K., 2007. Synthesis of a clinoptilolite-Fe system with high Cu sorption capacity. Chemosphere 67, 731–740. https://doi.org/10.1016/j.chemosphere.2006.10.072.

El-Azim, H., Mourad, F., 2018. Removal of heavy metals Cd (II), Fe (III) and Ni (II), from aqueous solutions by natural (clinoptilolite) zeolites and application to industrial wastewater. Asian J. Environ. Ecol. 7, 1–13. https://doi.org/10.9734/ajee/2018/41004.

Favvas, E.P., Tsanaktsidis, C.G., Sapalidis, A.A., Tzilantonis, G.T., Papageorgiou, S.K., Mitropoulos, A.C., 2016. Clinoptilolite, a natural zeolite material: structural characterization and performance evaluation on its dehydration properties of hydrocarbon-based fuels. Microporous Mesoporous Mater. 225, 385–391. https://doi.org/10.1016/j.micromeso.2016.01.021.

George, S., Pandit, P., Gupta, A.B., 2010. Residual aluminium in water defluoridated using activated alumina adsorption - modeling and simulation studies. Water Res. 44, 3055–3064. https://doi.org/10.1016/j.watres.2010.02.028.

Gomez, M.L., Blarasin, M.T., Martínez, D.E., 2009. Arsenic and fluoride in a loess aquifer in the central area of Argentina. Environ. Geol. 57, 143–155. https://doi.org/10.1007/s00254-008-1290-4.

Guaya, D., Valderrama, C., Farran, A., Armijos, C., Cortina, J.L., 2015. Simultaneous phosphate and ammonium removal from aqueous solution by a hydrated aluminum oxide modified natural zeolite. Chem. Eng. J. 271, 204–213. https://doi.org/10.1016/J.CEJ.2015.03.003.

Habuda-Stanić, M., Ravančić, M., Flanagan, A., 2014. A review on adsorption of fluoride from aqueous solution. Materials 7, 6317–6366. https://doi.org/10.3390/ma7096317.

Horst, M.F., Alvarez, M., Lassalle, V.L., 2016. Removal of heavy metals from wastewater using magnetic nanocomposites: analysis of the experimental conditions. Separ. Sci. Technol. 51, 550–563. https://doi.org/10.1080/01496395.2015.1086801.

Horst, M.F., Pizzano, A., Spetter, C., Lassalle, V., 2018. Magnetic nanotechnological devices as efficient tools to improve the quality of water: analysis on a real case. Environ. Sci. Pollut. Res. 25, 28185–28194. https://doi.org/10.1007/s11356-018-2847-8.

Kobayashi, Y., Ogata, F., Nakamura, T., Kawasaki, N., 2020. Synthesis of novel zeolites produced from fly ash by hydrothermal treatment in alkaline solution and its evaluation as an adsorbent for heavy metal removal. J. Environ. Chem. Eng. 8, 103687. https://doi.org/10.1016/j.jece.2020.103687.

Mohapatra, M., Anand, S., Mishra, B.K., Giles, D.E., Singh, P., 2009. Review of fluoride removal from drinking water. J. Environ. Manag. 91, 67–77. https://doi.org/10.1016/j.jenvman.2009.08.015.

Mondal, P., George, S., 2015. A review on adsorbents used for defluoridation of drinking water. Rev. Environ. Sci. Biotechnol. 14, 195–210. https://doi.org/10.1007/s11157-014-9356-0.

Mozgawa, W., 2000. The influence of some heavy metals cations on the FTIR spectra of zeolites. J. Mol. Struct. 555, 299–304. https://doi.org/10.1016/S0022-2860(00)00613-X.

Nakhli, S.A.A., Delkash, M., Bakhshayesh, B.E., Kazemian, H., 2017. Application of zeolites for sustainable agriculture: a review on water and nutrient retention, water, air, and soil pollution. Water, Air, Soil Pollut. https://doi.org/10.1007/s11270-017-3649-1.

Nie, Y., Hu, C., Kong, C., 2012. Enhanced fluoride adsorption using Al (III) modified calcium hydroxyapatite. J. Hazard Mater. 233–234, 194–199. https://doi.org/10.1016/j.jhazmat.2012.07.020.

Paoloni, J.D., Fiorentino, C.E., Sequeira, M.E., 2003. Fluoride contamination of aquifers in the southeast subhumid pampa, Argentina. Environ. Toxicol. 18, 317–320. https://doi.org/10.1002/tox.10131.

Pavelić, K., Hadžija, M., Bedrica, L., Pavelić, J., Crossed D signikić, I., Katić, M., Kralj, M., Bosnar, M.H., Kapitanović, S., Poljak-Blaži, M., Križanac, Š., Stojković, R., Jurin, M., Subotić, B., Čolić, M., 2000. Natural zeolite clinoptilolite: new adjuvant in anticancer therapy. J. Mol. Med. 78, 708–720. https://doi.org/10.1007/s001090000176.

Rahmani, A., Nouri, J., Kamal Ghadiri, S., Mahvi, A.H., R, Z.M., 2010. Adsorption of fluoride from water by Al3+ and Fe3+ pretreated natural Iranian zeolites. Int. J. Environ. Res. 4, 607–614.

Ruiz, R.L., Francisca, F.M., 2017. Remoción de flúor en agua mediante adsorción en suelos residuales. Fac. Ciencias Exactas Físicas y Nat.

Russo, V., Toriggia, L.F., Jacobo, S.E., 2014. Natural clinoptilolite – zeolite loaded with iron for aromatic hydrocarbons removal from aqueous solutions[1] V. Russo, L. F. Toriggia, and S. E. Jacobo, "Natural clinoptilolite – zeolite loaded with iron for aromatic hydrocarbons removal from aqueous sol. J. Mater. Sci. https://doi.org/10.1007/s10853-013-7741-7.

Sakhare, N., Lunge, S., Rayalu, S., Bakardjiva, S., Subrt, J., Devotta, S., Labhsetwar, N., 2012. Defluoridation of water using calcium aluminate material. Chem. Eng. J. 203, 406–414. https://doi.org/10.1016/j.cej.2012.07.065.

Salem Attia, T.M., Hu, X.L., Yin, D.Q., 2014. Synthesised magnetic nanoparticles coated zeolite (MNCZ) for the removal of arsenic (As) from aqueous solution. J. Exp. Nanosci. 9, 551–560. https://doi.org/10.1080/17458080.2012.677549.

Samatya, S., Yüksel, Ü., Yüksel, M., Kabay, N., 2007. Removal of fluoride from water by metal ions (Al3+, La3+ and ZrO2+) loaded natural zeolite. Separ. Sci. Technol. 42, 2033–2047. https://doi.org/10.1080/01496390701310421.

Scheverin, V.N., Horst, M.F., Russo, A.V., Jacobo, S., Lassalle, V.L., 2019. Síntesis y caracterización de nanocompuestos zeolita-magnetitas. XXXII Congr. Argentino Química.

Sujana, M.G., Pradhan, H.K., Anand, S., 2009. Studies on sorption of some geomaterials for fluoride removal from aqueous solutions. J. Hazard Mater. 161, 120–125. https://doi.org/10.1016/j.jhazmat.2008.03.062.

Sun, Y., Fang, Q., Dong, J., Cheng, X., Xu, J., 2011. Removal of fluoride from drinking water by natural stilbite zeolite modified with Fe(III). Desalination 277, 121–127. https://doi.org/10.1016/J.DESAL.2011.04.013.

Teutli-Sequeira, A., Martínez-Miranda, V., Solache-Ríos, M., Linares-Hernández, I., 2013. Aluminum and lanthanum effects in natural materials on the adsorption of fluoride ions. J. Fluor. Chem. 148, 6–13. https://doi.org/10.1016/J.JFLUCHEM.2013.01.015.

Tran, H.N., You, S.J., Hosseini-Bandegharaei, A., Chao, H.P., 2017. Mistakes and inconsistencies regarding adsorption of contaminants from aqueous solutions: a critical review. Water Res. 120, 88–116. https://doi.org/10.1016/j.watres.2017.04.014.

Viswanathan, N., Meenakshi, S., 2008. Enhanced fluoride sorption using La(III) incorporated carboxylated chitosan beads. J. Colloid Interface Sci. 322, 375–383. https://doi.org/10.1016/j.jcis.2008.03.007.

Waghmare, S., Arfin, T., Rayalu, S., Lataye, D., Dubey, S., 2015. Adsorption behaviour of modified zeolite as novel adsorbents for fluoride removal from drinking Water : surface phenomena. Kinetics and Thermodynamics Studies 4, 4114–4124.

World Health Organization, 2011. Guidelines for Drinking-Water Quality.

Xu, Q., Li, W., Ma, L., Cao, D., Owens, G., Chen, Z., 2020. Simultaneous removal of ammonia and phosphate using green synthesized iron oxide nanoparticles dispersed onto zeolite. Sci. Total Environ. 703, 135002. https://doi.org/10.1016/J.SCITOTENV.2019.135002.

Zhang, Z., Tan, Y., Zhong, M., 2011. Defluorination of wastewater by calcium chloride modified natural zeolite. Desalination 276, 246–252. https://doi.org/10.1016/J.DESAL.2011.03.057.